Multisensor Smart Eyewear for Biomarkers Acquisition

Ilaria Crupi, *Graduate Student Member, IEEE*, Alice Scandelli, *Graduate Student Member, IEEE*, Andrea Giudici, *Member, IEEE*, Giacomo Gervasoni, Diana Trojaniello, and Federica Villa, *Member, IEEE*

***Abstract*—The rapid evolution of smart eyewear technologies is opening new frontiers across various fields. Thanks to their proximity to highly vascularized facial areas and access to all five senses, smart glasses offer a unique opportunity to acquire key physiological and behavioral biomarkers, enabling health monitoring while preserving wearability. In particular, the proposed system targets cardiorespiratory parameters [such as heart rate (HR) and blood oxygen saturation] and activity monitoring (such as gait analysis and human activity recognition). This work presents the development of a multisensor platform able to acquire different biomedical signals, designed to be embedded into a regular eyewear prototype. This standalone system is powered by a 200-mAh, 3.7-V LiPo battery and comprises three printed circuit boards (PCBs) that integrate sensors for photoplethysmography, electrocardiography, inertial measurements, and capacitive sensing. The device also performs local data storage and wireless data transmission, allowing for flexible use in offline data collection as well as real-time communication with external systems. Two use cases are presented to demonstrate the device's ability to continuously capture physiological signals for approximately 8 h and to extract health-related metrics in real time, validating its use for real-life applications in continuous health monitoring.**

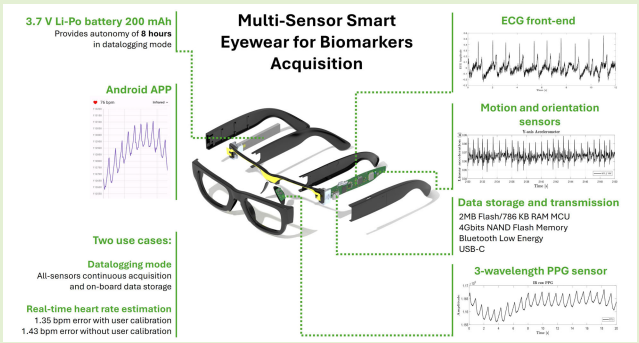

***Index Terms*— Biomedical signals acquisition, continuous physiological monitoring, embedded systems, smart eyewear.**

I. Introduction

THE term *smart eyewear* refers to an emerging class of head-mounted devices that integrates sensing, advanced data processing, and communication capabilities into an eyeglass form. The current smart eyewear portfolio includes a wide range of devices, from microphone- and Bluetooth-enabled glasses (e.g., Ray-Ban Stories [1]) to immersive augmented reality (AR) glasses (e.g., Meta Orion [2]). Advancements in technology and artificial intelligence (AI) have further expanded the potential of smart eyewear, enabling the integration of intelligent algorithms and complex processing directly into the device (e.g., Ray-Ban Meta AI glasses [3]). As a consequence, the demand for innovation and advanced features grows, and the adoption of smart glasses is expected to rise significantly, with an anticipated average annual growth rate of 29.4% [4].

What sets smart eyewear apart from other wearables is its ability to engage all five senses, thanks to its strategic position on the head and proximity to eyes, ears, and brain. While this positioning contributes to a more enhanced user experience, it also presents a unique opportunity for unobtrusive health monitoring. By integrating sensors capable of tracking biomarkers, smart eyewear could extend beyond currently available applications in consumer and industrial settings, unlocking entirely new use cases in personal health and wellbeing.

Received 7 July 2025; revised 11 September 2025; accepted 22 September 2025. Date of publication 3 October 2025; date of current version 31 October 2025. This work was supported by the EssilorLuxottica Smart Eyewear Laboratory, a Joint Research Center between EssilorLuxottica and Politecnico di Milano. The associate editor coordinating the review of this article and approving it for publication was Dr. Hailing Fu. *(Ilaria Crupi and Alice Scandelli contributed equally to this work.) (Corresponding author: Federica Villa.)*

This work involved human subjects or animals in its research. Approval of all ethical and experimental procedures and protocols was granted by Approval of all ethical and experimental.

Ilaria Crupi, Alice Scandelli, Andrea Giudici, and Federica Villa are with the Dipartimento di Elettronica, Informazione e Bioingegneria, Politecnico di Milano, 20133 Milan, Italy (e-mail: ilaria.crupi@polimi.it; alice.scandelli@polimi.it; andrea.giudici@polimi.it; federica.villa@polimi.it).

Giacomo Gervasoni and Diana Trojaniello are with the EssilorLuxottica Smart Eyewear Laboratory, EssilorLuxottica, 20123 Milan, Italy (e-mail: giacomo.gervasoni@luxottica.com; diana.trojaniello@luxottica.com).

Digital Object Identifier 10.1109/JSEN.2025.3614692

A. Motivations

The advantageous positioning of smart eyewear allows access to unique areas of the head where multiple biosignals can be acquired without causing discomfort to the user. Thanks to the weight and the design of the eyeglasses themselves, biosensing components can be placed on specific contact points of the head that remain in constant touch with the skin, enabling the acquisition of biomedical signals that require skin contact, such as photoplethysmogram (PPG), electrocardiogram (ECG), bioimpedance (BioZ), and electrodermal activity (EDA). Notable sensor placement areas in eyewear and googles include the nose pads, the forehead, and the temple ear bends [5]. In addition, motion sensors can be integrated in other parts of the frame, such as the temple fronts, enabling the detection of specific head movements and general activities like walking and running [5].

Due to its singular position, smart eyewear also enables the acquisition of biosignals related to ocular and brain activity, such as electrooculography (EOG) and electroencephalography (EEG) [5]. These additional capabilities expand the traditional physiological monitoring in wearables, enabling new interaction modalities and cognitive state assessments.

Furthermore, differently from the wrist, the head can be a more stable measurement site, providing motion-resilient physiological signals [6].

B. Related Works

In recent years, several studies have explored the feasibility of acquiring biosignals directly from the head, leveraging its strategic position. Some devices have been specifically designed in the form of smart eyewear, while others have exploited already existing head-mounted devices such as virtual reality (VR) or AR headsets. However, despite the increasing interest in this field, many existing solutions still face limitations in terms of size, power consumption, and onboard processing capabilities.

To contextualize our work, this section will: 1) provide a brief overview of the biosignals that are acquired from the head and their measurement points; 2) analyze the state of the art of eyewear-based biosensing devices, focusing on their hardware, data processing, and power efficiency; and 3) discuss the main limitations of current solutions and explain how our approach represents an innovation compared to existing devices.

1) Biosignals Acquisition From the Head: Due to its strategic position and the stable contact points provided by smart eyewear, the head holds great potential for physiological signal acquisition. Here, we will analyze the most relevant as follows.

1) *PPG:* The PPG signal is widely used both in wearable devices and in clinical settings to monitor heart rate (HR), HR variability (HRV), blood oxygen saturation (SpO2), breathing rate (BR), and also for autonomic function evaluation and vascular assessment [7], [8]. It requires the use of a light source, usually a light-emitting diode (LED), and a photodiode (PD) for measuring the light reflected by the tissues. The head is a highly vascularized body area, primarily supplied by the internal and external carotid arteries. Their branches extend to the nose, temples, and ears, making these locations particularly suitable for acquiring the PPG signal [9]. Previous studies have demonstrated the feasibility of extracting the PPG signal from multiple positions on the head, such as the nose [10], [11], [12], forehead [13], temples [14], auricular region [15], and ear canal [16]. All these areas are characterized by a bony structure covered by thin skin layers, which contributes to considerable backscattering of the incident light, thereby enabling a strong reflective PPG signal. As a result, head-mounted devices with built-in PPG sensors represent a suitable, cost-effective method for measuring multiple vital signs in a straightforward way.
2) *Inertial Signals and Head Motion Analysis:* Inertial signals, such as linear accelerations and angular rotations, consist of tri-axial measurements captured by inertial measurement units (IMUs). In the healthcare domain, IMUs are widely used in wearable devices to track movement patterns, estimate spatiotemporal gait parameters, assess physical activity, predict energy expenditure, and detect falls [17]. Head-worn devices are less prone to positional variations compared to other devices, such as smartphones [18], and the head is considered a valuable site for extracting information related to the user's activity [19]. In this context, IMUs are typically embedded in ear-worn devices [20], VR headsets [21], or temple arms of smart glasses [18]. Head-mounted inertial sensing has been successfully employed for gait analysis [20], [22], movement tracking, and step counting [19], [23]. Furthermore, the high sensitivity of these sensors enables the detection of microhead movements associated with cardiac contraction and respiration [21], [24], making them also suitable for unobtrusive cardiorespiratory monitoring.
3) *EOG:* EOG is a technique used to measure eye movements by detecting the corneoretinal potential through electrodes placed near the eyes. Recent studies with smart eyewear demonstrate the feasibility of acquiring EOG using electrodes placed on the nose pads, nose bridge, and temple tips, and consequently to monitor gaze direction, blink rate, and cognitive load [23]. This information is useful for enhancing human–machine interaction and providing users with insights into their mental state, attention level, and drowsiness [25].
4) *EEG:* EEG is a noninvasive approach used to record brain electrical activity by means of electrodes placed on the scalp. Recent developments have enabled the integration of electrodes along headbands and eyewear-based devices [25], [26], allowing for the monitoring of user engagement during specific tasks and learning activities.
5) *Electromyography (EMG):* EMG measures the electrical activity of skeletal muscles. The head is particularly well suited for such measurement due to the presence of the temporalis and masseter muscles, which are involved in mastication [27]. As shown in [27], bilateral electrodes placed around the ears can effectively detect chewing

and eating activity, supporting applications in dietary monitoring.

6) *EDA:* EDA is the measurement of skin conductance by applying a small dc voltage across two electrodes. This technique provides insights into emotional arousal driven by the sympathetic nervous system. Several studies have demonstrated the feasibility of acquiring EDA signals from the forehead, the temples, and behind the ears, enabling the estimation of parameters related to emotional arousal, stress levels, and the detection of microsleep episodes [28], [29].

2) Existing Smart Eyewear for Biosensing: Several studies have proposed hardware solutions for biosignal acquisition using head-mounted devices. For instance, Siddharth et al. [30] presented a wearable multimodal biosensing headset integrating PPG, EEG, eye–gaze tracking, motion capture, and GSR for real-world applications. Similarly, Ferlini et al. [6] discussed the opportunities and challenges of mobile health with head-worn devices, including smart glasses and earbuds equipped with multiple sensors for cardiovascular, neurological, and behavioral monitoring.

In this work, we focus on devices with an eyewear form factor. Some of these are presented here with a focus on sensor integration, data processing methods, and power consumption.

1) *Pulse-Glasses [11]:* This prototype consists of a 3-D-printed frame embedding a one-wavelength (green) PPG sensor into the nose pad. The left temple houses a printed circuit board (PCB) featuring an ATmega32U4 microcontroller unit (MCU) and a Nordic nRF8001 Bluetooth low energy (BLE) chip for wireless communication with an Android app. A rechargeable 3.7-V, 300-mAh lithium-ion battery is integrated into the right temple to power the system.
2) *Glabella [12]:* Glabella integrates three one-wavelength (green) PPG sensors (one on the nose pad and two on a temple) along with a three-axis accelerometer for motion artifact compensation. Data are acquired and locally processed using an ARM Cortex-M3 MCU. Data can also be stored on a micro secure digital (SD) card for offline analysis. Powered by a 305-mAh LiPo battery, the system supports approximately 15 h of continuous acquisition.
3) *Toral's Prototype [13]:* This device includes three ECG electrodes, a dual-wavelength red and infrared (IR) PPG sensor placed at the temple, and a six-axis IMU. A PSoC5LP MCU handles signal acquisition and processing, while a BLE module transmits data wirelessly. A 100-mAh battery powers the system for over 2 h and 20 min with all sensors active, and for more than 1200 h in sleep mode. Power requirements vary depending on function: 74 mW for a 30-s ECG recording, and 105 mW for a 20-s SpO_2 measurement.
4) *AttentivU [26]:* This system delivers auditory feedback through bone conduction. The device includes two PCBs hosting an MCU, a Bluetooth module, a power management system, two EEG electrodes, two EOG electrodes, and one reference electrode. It is powered by a 3.7-V, 150-mAh LiPo battery, allowing for about 5 h of operation, with an average current draw of ∼30 mA. It also has the possibility to connect an external battery and extend usage up to 15 h.
5) *SPIDERS+ [31]:* This advanced eyewear embeds an IR camera, a proximity sensor, and a six-axis IMU. These sensors are used to capture facial and eye movements, pupillometry, zygomaticus muscle activity, and head motion. The device integrates two PCBs and uses an ESP32 module (by Espressif) for Wi-Fi and Bluetooth communication. The onboard battery is a 2000-mAh unit, with up to 9 h of usage. Power consumption varies from 5 mW in sleep mode to 760–839 mW during full data acquisition and transmission. This platform supports real-time and semi-real-time processing, and its capabilities can be further expanded with additional boards embedding a PPG sensor and an eight-channel EEG sensing.

The aforementioned devices represent valuable examples of electronic integration within eyewear, enabling the acquisition and processing of physiological data from the head. However, when considering key requirements such as wearability, sensor integration, measured signals, power consumption, and autonomy, each solution inevitably presents at least one limitation. None of the existing devices manages to optimally balance all these key aspects of an advanced eyewear-based sensing platform. Some of the previously presented devices require additional modules or external battery packs, compromising usability and resulting bulky design because of the large housings placed in the temples [13], [26], [31]. Some of them are instead lacking fully integrated sensors within the frame, further impacting wearability [13], [31]. High power consumption and the absence of fully standalone functionality are also recurrent limitations, as many of the presented examples require frequent charging or a connection to external devices such as smartphones or computers for data storage and processing [11], [13]. Finally, even if standalone and able to perform in-the-wild evaluations, some of the devices' measurement capabilities are limited to few signals, such as only the PPG signal and the head accelerations [12] or only EOG and EEG [26].

Our work aims to overcome these limitations by developing a multisensor platform that combines wearability, standalone operation, and power efficiency, and that can be fully integrated into a regular eyewear prototype.

II. Hardware Design

The design of a multisensor smart eyewear system must satisfy several requirements in terms of: 1) dimensions, the size must be small to fit inside a standard glass frame and light enough to avoid discomfort when worn; 2) power consumption, since the smart eyewear is intended to operate for at least an entire day, the battery constraint becomes a key consideration, still ensuring proper functioning and continuous monitoring of physiological parameters; and 3) sensors placement, indeed, according to the measured signal, the placement of the sensor can be crucial, for example, PPG sensors require stable contact with the user's skin for accurate measurement.

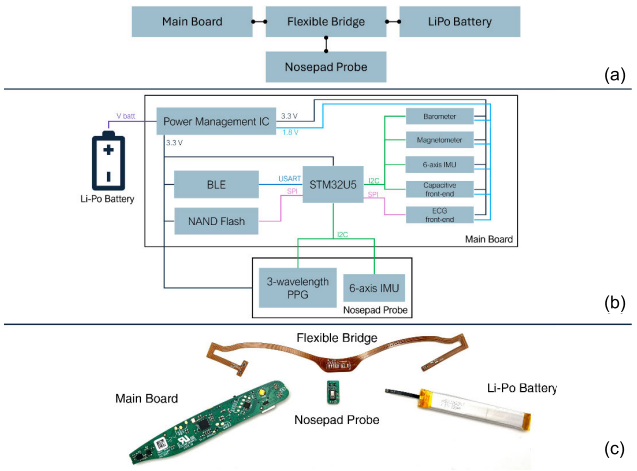

Fig. 1. (a) General block diagram of the proposed multisensor smart eyewear. It is composed of three PCBs and the LiPo battery. All four parts are electrically connected together via specific connectors or via soldering. (b) Detailed description of the components, the connection between them, and power delivery. (c) Pictures of all the elements.

Fig. 2. Fully assembled system embedded into a standard eyewear frame. The green LED light from the PPG sensor placed on the left nose pad is clearly visible (Left). Partially disassembled view, showing the integration of the main board on the left temple and the nose pad probe on the left nose pad (Right).

A. Overall System Description

Fig. 1 shows the single parts that compose the proposed system. This is made of three PCBs: a main board, a flexible bridge and a nose pad probe, and the LiPo battery, connected via Hirose connectors or via soldering pads.

All the boards are designed to be integrated in a glass frame developed ad hoc for the system (Fig. 2). In particular, the main board is placed inside the left temple, the flexible bridge runs along the frontal part of the frame, and it connects to the battery on the right temple and to the nose pad probe on the eyewear bridge. To ensure mechanical stability, soldering robustness, and higher component density, rigid PCBs were chosen for most parts of the system. Only where bending is strictly required by the frame shape (i.e., rim and hinges), flexible printed circuits are used.

The main board hosts an MCU, communication interfaces, a flash memory, sensors, and sensor front end. The nose pad probe hosts a three-wavelength PPG sensor and a six-axis IMU. The battery has a capacity of 200 mAh and a nominal voltage of 3.7 V, supporting long-lasting system operation. Table I lists the parameters that can be extracted from each sensor present in the system.

B. Main Board

The selection of components for the main board was primarily driven by two main characteristics: small package sizes and low power consumption but also by the necessity to test and debug it.

TABLE I
LIST OF PARAMETERS THAT CAN BE EXTRACTED FROM THE SENSORS PRESENT IN THE SYSTEM

Sensor	Signals	Extracted Parameters
IMU 6-axis	Linear accelerations Angular rotations	Step counting [20], gait analysis [20], HR from ballistocardiogram [24], HAR [32].
Magnetometer	Magnetic field	HAR and indoor positioning [33].
Barometer	Atmospheric pressure	Changes in user elevation and HAR [34].
ECG front-end	ECG	HR, HRV, heart activity analysis [35].
Capacitive front-end	Variation in capacitance between electrodes	Worn status, user interface, expression detection [36], eye tracking, EOG [37].
PPG	PPG	HR [11], blood oxygen saturation [38], blood pressure [12].

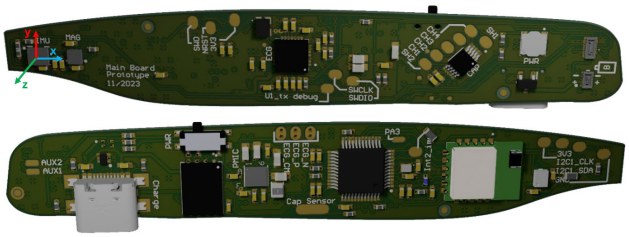

Fig. 3. Three-dimensional render of the main PCB, front, and back. In the upper image, the orientation of the three-axis IMU is highlighted.

The number of components and their package were chosen as a tradeoff between space constraints to fit an eyewear frame and the accessibility for debug and test the most critical components, such as the MCU, the communication peripherals, and the power management integrated circuit (PMIC), resulting into a total area of 1207 mm^2 with 124 components and a density of 43.21%. A picture of the front and back of the main board is shown in Fig. 3. The main board hosts an MCU from STMicroelectronics' U5 family, selected for its low-power functionalities. In addition, a PMIC provides efficient power management, handling battery charging, programmable power rails, and supporting both 1.8- and 3.3-V outputs for the board's components. This integrated circuit (IC) integrates a fuel gauge algorithm, monitoring current consumption during system operations. The board also interfaces with a PC via USB-C for recharging and data exchange and enables wireless connectivity through a BLE module from Microchip. From a sensing and user interaction perspective, it integrates multiple components for data acquisition, processing, and debugging.

1) *Data Storage:* A serial peripheral interface (SPI) NAND flash memory (4 Gbit) for local data storage.
2) *Sensor Front Ends:* Two ICs dedicated to capacitive sensing and ECG acquisition.
3) *Sensors:* A magnetometer, a barometer (with temperature sensing), and a six-axis IMU.
4) *User Interface:* A slide switch for power on/off control and an RGB LED on the external side of the board for visual feedback.
5) *Debug:* Some pads are provided for accessing the MCU's debug mode via serial wire output (SWO).

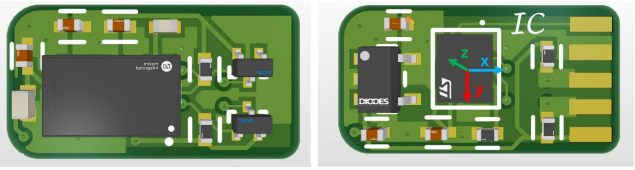

Fig. 4. Three-dimensional rendering (top and bottom) of the PPG probe, designed to be placed in the left nose pad. In the right image, the orientation for the three-axis IMU is shown for reference.

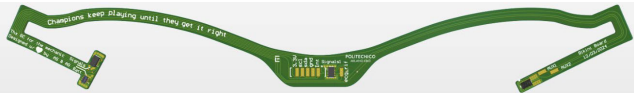

Fig. 5. Three-dimensional rendering of the flexible PCB for routing the signals from the main board to the nose pad and for connection with the battery placed on the opposite temple.

All ICs are connected to the MCU via inter-IC (I^2C) or SPI communication lines, while the BLE module implements a transparent universal asynchronous receiver–transmitter (UART) communication.

C. Nose Pad Probe

A custom PPG probe, designed to acquire the PPG signal from the head [39], was connected to the flexible bridge and placed on the left nose pad of the eyewear frame, since this position was identified to be the best one in [9]. The probe comprises a PPG sensor featuring three integrated LEDs (red, IR, and green) and a PD, and a high-performance six-axis IMU that embeds a machine learning core (MLC) (Fig. 4).

D. Flexible Bridge

The connection between all the boards in the system and the battery is ensured by the presence of a PCB made in flexible technology (Fig. 5). The shape of this board was made ad hoc to be integrated into the frontal part of the glass frame and hosts three connectors to interface with the main board, the nose pad probe, and the battery.

III. Firmware and Software Development

This paragraph presents the general configuration of the main components mounted on the system. Then, two application examples are introduced: datalogging and real-time HR estimation.

A. General Configuration

At system start-up, the PMIC powers all circuit sections. The power rail voltages are initially defined by the PMIC's one-time programmable (OTP) memory values, which are not optimal in terms of system efficiency and performance. To address this, the MCU reconfigures the PMIC via the I^2C interface, adjusting its registers to generate the correct voltage levels necessary for proper and efficient board operation. Specifically, two distinct voltages, 3.3 and 1.8 V, are generated through the two integrated LDOs.

Once the power rails are correctly established, the BLE module is configured in transparent UART mode, functioning as a serial bridge that relays data from the host (the MCU) to a remote device, without adding protocol overhead.

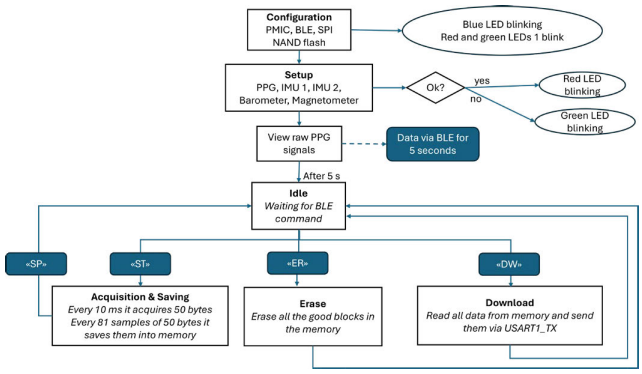

Fig. 6. General scheme of the firmware developed for data logging. It is organized into six main states: configuration, setup, idle, acquisition and saving, erase, and download. Some states are sequential and triggered by timers, while others can be triggered by the user via BLE commands.

Subsequently, the nonmanaged NAND flash memory is initialized via the SPI protocol, ensuring proper handling of bad and good blocks and enabling error correction control. Although nonmanaged memory entails additional firmware overhead, it occupies significantly less board area compared to managed memory solutions such as eMMC.

Following this general configuration, two use cases, i.e., datalogger and real-time HR estimation, were identified and are described in Sections III-B and III-C.

B. Datalogger

The firmware for the data logging application is designed to manage the acquisition of all system sensors, the storage of collected data in the embedded flash memory, and the transmission of this data to an external device (PC) for further analysis. This setup supports the generation of datasets suitable for advanced feature extraction or for training AI-based models. The firmware operates through six distinct states, activated by either timers or external BLE inputs, as summarized in the general workflow depicted in Fig. 6.

Initially, the system performs the *configuration* phase described in Section III-A. Once the PMIC, BLE, and NAND flash memory are configured, the system proceeds with the setup of the sensors. These are sequentially configured according to the parameters shown in Table II. Upon successful configuration, a green LED blinks three times at 2 Hz; if configuration fails, a red LED blinks in the same manner.

Setup is a brief phase for signal verification. For five seconds, PPG signals are sampled at 50 Hz and transmitted over BLE for real-time visualization on a custom Android application, as detailed in Section III-C.2. This functionality allows the user to assess the correct placement of the eyewear frame by visually inspecting the PPG signals.

After this initial check, the system enters an *idle* state, during which it awaits commands from the Android app via BLE. When the "ST" (START) command is received, the system transitions into *acquisition* mode. In this state, a timer interrupt at 100 Hz initiates timestamping via the MCU's internal RTC, acquisition of sensor data, and data storage. Each data packet is composed of 5 bytes for the timestamp, 9 bytes for PPG signals (three channels, 3 bytes each), 24 bytes for accelerometer and gyroscope data (6 bytes each for two

TABLE II
SENSOR SETTINGS APPLIED DURING THE SETUP STATE FOR THE "DATALOGGER" USE CASE

Sensor	Output Data Rate [Hz]	Other settings
MAX30101 (PPG sensor)	200	Peak current: 6 mA Pulse width: 411 µs ADC resolution: 18 bit
LSM6DSV16BX (Nosepad IMU)	240	Linear acceleration full scale: ±8 g Angular rate full scale: ±1000 dps
LSM6DSO16IS (Main Board IMU)	208	Linear acceleration full scale: ±8 g Angular rate full scale: ±1000 dps
IIS2MDC (magnetometer)	100	Dynamic range: ±50 Gauss
DPS310 (barometer)	100	Resolution: 2.5 Pa_{RMS} Resolution: 0.01 °C

IMUs), 6 bytes for magnetometer data, and 3 bytes each for barometric pressure and temperature readings. This results in a total of 50 bytes every 10 ms (5 kB/s on average). Data are buffered and written to memory once 4096 bytes, equivalent to one memory page, are accumulated, approximately every 810 ms. The total memory capacity of 4 Gbit allows for up to 29 h of continuous data acquisition. When the "SP" (STOP) command is issued, acquisition is halted, remaining data are saved, and the system returns to the idle state.

In addition to acquisition, the firmware includes a memory management state. Upon receiving the "ER" (ERASE) command via BLE, the system resets all good blocks in the SPI NAND flash memory and subsequently returns to the idle state.

Data download is initiated by the "DW" (DOWNLOAD) command. In this mode, stored data are read from memory and transmitted via USB to a connected PC. Once the entire dataset has been sent, the system reverts to idle. On the PC, a dedicated Python script decodes the binary data, reconstructs the sensor values, and saves them in a.csv file for further offline processing.

C. Real-Time HR Estimation

1) Firmware: The second firmware allows for continuous PPG signal acquisition, real-time HR estimation, and data streaming via BLE. This use case targets real-time applications requiring live physiological feedback; thus, it is ideal for immediate health monitoring feedback and tracking systems. To enhance modularity and readability, the MCU main code was structured as a finite state machine with five states: start-up, *setting*, *not worn*, *calibration*, and *acquisition* (Fig. 7). For the last three states, a unique identifier is transmitted via BLE to indicate the current state: "NW" for *not worn*, "C" for *calibration*, and "A" for *acquisition*. In addition, "B" is sent to indicate the battery state of charge and charging status. These characters help the receiver interpret both the system state and battery information in real time.

At power-up, the MCU performs initial configurations and verifies communication with the PPG sensor; upon success, it proceeds to configure the sensor by setting parameters such

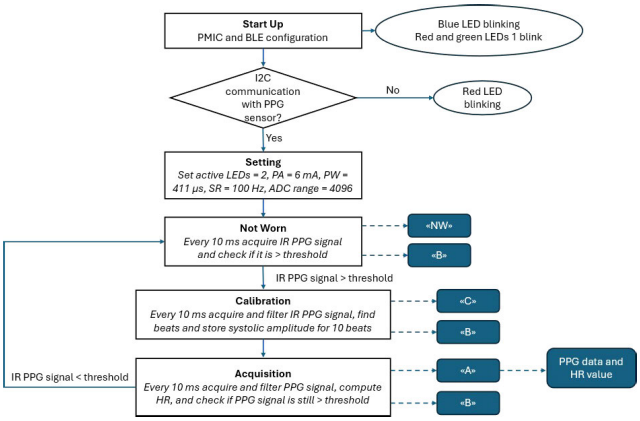

Fig. 7. General scheme of the firmware developed for real-time HR estimation. It is organized into five main states: start-up, setting, not worn, calibration, and acquisition. For the last three states, unique characters are transmitted via BLE, along with the battery status.

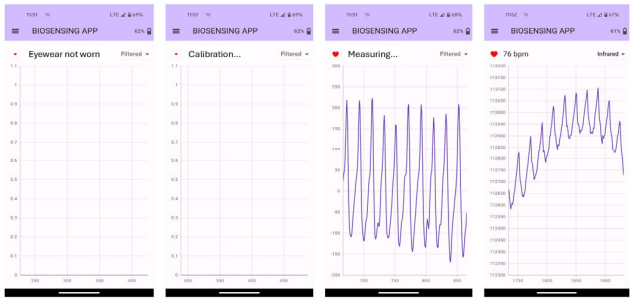

Fig. 8. Four screens of the mobile Android app, showing the different statuses in the real-time heart rate estimation application example.

as number of active LEDs, pulse amplitude (PA), pulsewidth (PW), sample rate (SR), and internal ADC range. The *not worn* state monitors whether the eyewear is being worn by using the PPG sensor as a proximity sensor, i.e., evaluating the PPG signal values against a predefined threshold. When the eyewear is detected as worn, an optimized version of the custom function presented in [39] is used to tailor the HR estimation algorithm to the specific user. During this phase, the PPG systolic amplitude is stored over 10 beats, and the mean of these values is used to set the peak amplitude threshold for HR estimation. Since the amplitude of the acquired PPG signal highly depends on the subject's physiognomy, this approach adapts the algorithm to individual physiological variations and recalculates the threshold each time the eyewear is worn again, improving real-time HR accuracy. In the *acquisition* state, the PPG signal is acquired at 100 Hz and processed sample-by-sample to compute the HR in real time using the personalized threshold. The computed value is then transmitted via BLE, together with the raw PPG signal and filtered PPG signal. The system continuously monitors the PPG signal to ensure that the eyewear is still worn.

2) Android App: To enable real-time visualization of the acquired PPG signal and the estimated HR value, a simple Android app was developed (Fig. 8).

Upon launch, the app scans for nearby devices and establishes a connection with the eyewear's BLE module. Once connected, the main window displays a graph, the battery's state of charge, and a text box indicating the eyewear's status. If the eyewear is not being worn, the app displays a message

confirming this. When the user puts the eyewear on, the app shows that the calibration phase is in progress. After that, the app dynamically plots the PPG signal in real time, alongside the estimated HR value in beats per minute (bpm). In addition, the user can select between viewing the raw PPG signal or the filtered version, offering flexibility in data visualization based on their preferences or requirements.

IV. Results

A. Power Consumption

To analyze the power consumption of the system, a Keysight Technology 34465A digital multimeter was used to log a full battery discharge cycle while running the firmware described in Section III-A in the acquisition state, with all the sensors active and data being saved to memory. The primary contributor to power draw is the MCU, whose consumption scales linearly with the system clock frequency according to (1)

$$P = C \times V^2 \times f_{\mathrm{SYSCLK}} \tag{1}$$

where P is the dissipated power, C is the capacitance, V is the voltage supply, and f_{SYSCLK} is the system clock frequency.

A tradeoff analysis revealed that the system is constrained by memory read/write speed, requiring a minimum clock frequency of 55 MHz to complete both data acquisition and memory storage within the 10-ms cycle. The measurements showed an average current consumption of 25 mA, which corresponds to a battery life of approximately 8 h when using a 200-mAh battery, which is sufficient for a datalogger application in free-living protocols lasting a full working day.

B. Signals Acquisition in Datalogger Case

In this section, we present the results obtained using the datalogging firmware described in Section III-B. Fig. 9 presents an example of a dataset acquired during a dynamic protocol that included transitions between sitting, standing, and lying down, as well as cycling at varying intensities, walking, running, and ascending/descending stairs. Each phase was marked by a deliberate head rotation, which is distinctly visible in the IMU recordings. The six time-synchronized sensor traces in the figure illustrate data collected from the two six-axis IMUs placed at the temple and nose, and raw PPG signals (red, IR, and green), all recorded over approximately 1 h without interruptions. A zoomed-in view highlights a motion artifact, specifically a jump, occurring at around 3868 s. This artifact is clearly visible across all sensor traces, demonstrating precise synchronization between accelerometers, gyroscopes, and PPG channels.

In addition to the continuous sensors' recording presented here, the device also supports on-demand ECG acquisition from the head. This modality is currently not added to the datalogging firmware since ECG measurements require the user to actively place a finger on the eyewear's left temple, an action that cannot be sustained during continuous recordings.

This feature, instead, targets short ECG acquisitions that can complement PPG cardiovascular monitoring, if needed.

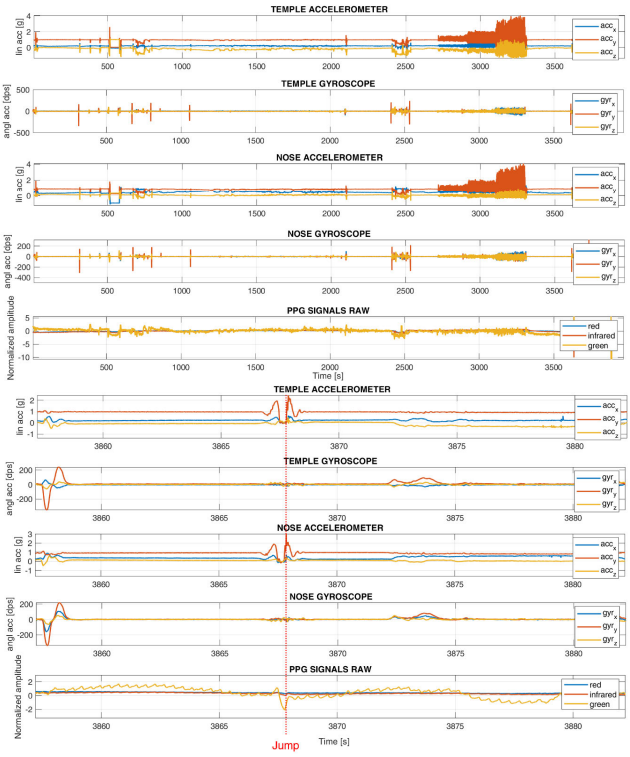

Fig. 9. Top: time-synchronized multisensor recording during a dynamic protocol (∼1 h), including IMUs and raw PPG signals from sensors at the temple and nose. Distinct activity phases (e.g., posture changes, cycling, walking, running, and stairs) are separated by head rotations visible in IMU data. Bottom: zoom on a jump artifact (∼3868 s), showing simultaneous response across all sensors, confirming precise channel synchronization.

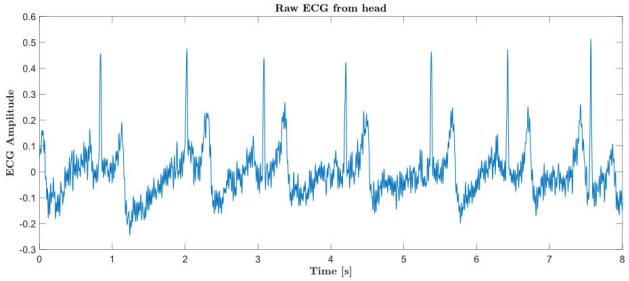

Fig. 10. Example of on-demand raw head ECG acquired with 256-Hz SR from the eyewear frame.

TABLE III
Preliminary Results of Instantaneous HR Estimation and Beat Detection for Each Subject, With and Without the Calibration Phase

Subject #	MAE STD (No Calibration) [bpm]	F1-Score (No Calibration)	MAE STD (Calibration) [bpm]	F1-Score (Calibration)
1	1.06 ± 0.66	1	0.68 ± 0.58	1
2	17.09 ± 19.86	0.78	8.25 ± 10.10	0.93
3	1.23 ± 1.20	1	1.19 ± 1.27	1
4	1.64 ± 1.44	1	1.52 ± 0.94	1

A dedicated study was conducted to find both the optimal electrodes' material and placement on the eyewear frame [40]. Fig. 10 shows an example of an ECG signal acquired with our eyewear prototype, presenting clear R-peaks and morphological features comparable to conventional chest ECG.

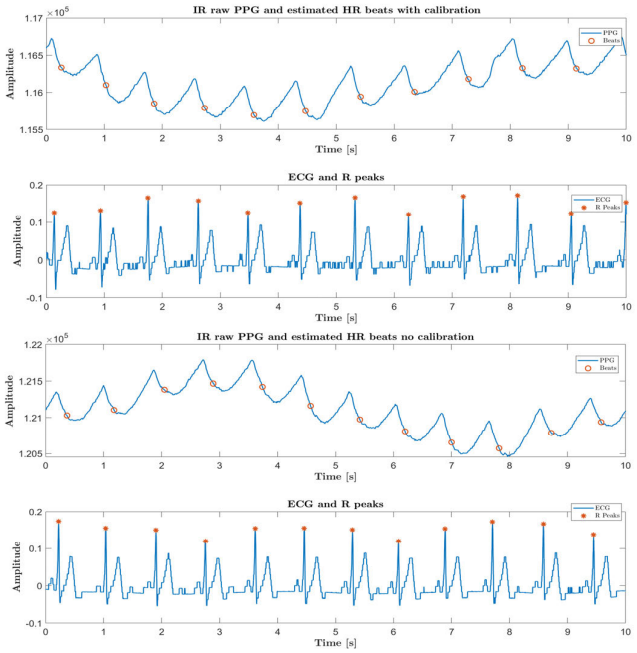

Fig. 11. Example of good quality raw IR PPG signal. All beats are correctly identified.

TABLE IV
COMPARISON OF OUR DEVICE WITH EXISTING EYEWEAR-BASED SYSTEMS IN TERMS OF BATTERY DURATION, INTEGRATION IN A STANDARD FRAME, AND NUMBER OF EMBEDDED SENSORS

Existing Devices	Battery Duration (> 7 h)	Standard frame	Types of sensors
[11]	N.A.	✓	PPG
[12]	✓	✓	PPG, 3-axis accelerometer
[13]	×	×	PPG, ECG front end, Accelerometer
[26]	×	×	EEG, EOG
[31]	✓	×	IR camera, proximity sensor, 6-axis IMU, PPG, EEG
Ours	✓	✓	PPG, ECG front-end, 6-axis IMU, barometer, magnetometer, capacitive front end

C. Real-Time HR Estimation Case

A preliminary evaluation of the impact of the calibration phase on beat detection, thus on HR estimation, was performed on 20-s PPG acquisitions collected from four subjects (two males, two females, and a mean age of 27.5 ± 2.5 years). All subjects provided voluntary written, informed consent to the experimental protocol, approved by the Ethical Committee of the Politecnico di Milano (date of approval: October 16, 2023, number 33/2023) in accordance with the Declaration of Helsinki of 1975, as revised in 2000. Each subject underwent two trials: one PPG measurement with the calibration phase enabled, and one without. For each acquisition, a concurrent three-lead ECG signal was acquired from the chest as the gold-standard. The PPG sensor was set with PA equal to 6 mA, 411-μs PW, and 100-Hz SR. The PPG raw data were transmitted via BLE to a serial terminal, together with a flag indicating whether a beat had been detected or not.

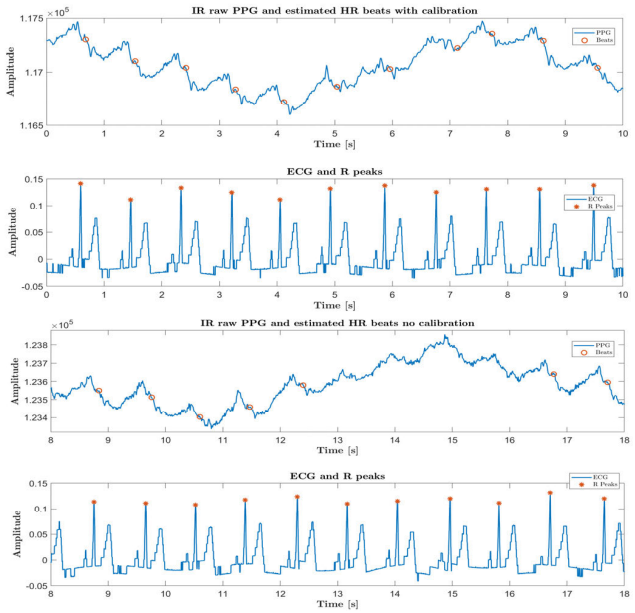

Fig. 12. Comparison between PPG and ECG signals in the cases with (top) and without (bottom) calibration. The raw IR PPG signal is shown along with the beats detected in real time by the MCU. The concurrent three-lead ECG signal is also shown along with the R-peaks identified in postprocessing. Calibration phase leads to improved beat detection, particularly in the presence of noisy PPG signals.

Table III lists the preliminary results obtained for each subject with and without the calibration phase. The accuracy of instantaneous HR estimation from PPG compared to the one obtained from the ECG reference signal is quantified by the mean absolute error (MAE) in bpm; the performance on beat detection, instead, is computed using the $F1$-score.

For most subjects, the PPG signals were of high quality, and calibration had minimal effect (Fig. 11). In contrast, subject 2 had a noisy PPG signal due to poor sensor and skin contact (Fig. 12), and calibration led to improved performance, suggesting that the optimized algorithm partially compensates for the reduced signal quality.

V. CONCLUSION

This article presents a compact, wearable multisensor system fully embedded within a standard eyewear frame, designed to enable unobtrusive physiological monitoring. The device incorporates a wide range of sensors, including a three-wavelength PPG sensor, two IMUs, a barometer, a magnetometer, a capacitive sensing front end, and an ECG analog front end, preserving wearability without requiring external modules or bulky housings. By combining multiple sensing modalities, full integration, and continuous operation, the system effectively addresses the key limitations of previous eyewear-based platforms (Table IV). As summarized in Table IV, our device differs from previously reported smart eyewear systems by simultaneously ensuring long-term operation (battery duration > 7 h), seamless integration into a standard frame, and the highest number of embedded sensors (six), thus enabling a more comprehensive monitoring of physiological and behavioral parameters.

The system supports both continuous onboard data logging and real-time signal processing, making it a versatile tool for a

wide range of applications, from long-term monitoring in free-living scenarios to real-time feedback in clinical or laboratory studies.

In the datalogging use case, the device presents about 8 h of battery life with all sensors on and the possibility to continuously store data for about 29 h. This enables continuous and synchronized data collection from a single, consistent point of measurement, improving reliability while reducing the complexity of experimental setups. Furthermore, the extensive onboard memory capacity allows for extensive datasets collection, aligning with the growing demand for large-scale data acquisition for machine learning and neural network applications.

For the real-time signal processing case, the device is able to continuously compute HR estimation from the PPG signal, and stream it to any external connected device together with the PPG signal itself. Preliminary 20-s acquisitions on four subjects showed a median MAE of 1.43 b/m without the calibration phase and 1.35 b/m with the calibration phase. Notably, the calibration phase can help in case of poor-quality PPG signals, as for subject 2, whose HR estimation showed a 51.7% improvement in MAE (from 17.09 to 8.25 b/m) when initial calibration was performed.

Future works will focus on further miniaturizing the electronics and on developing a user friendly graphical user interface to simplify sensor configuration and broaden accessibility, making it an even more powerful device for both research and real-life applications.

REFERENCES

[1] (Sep. 2021). *Introducing Ray-Ban Stories: First-Generation Smart Glasses*. [Online]. Available: https://about.fb.com/news/2021/09/introducing-ray-ban-stories-smart-glasses/

[2] (2024). *Orion AI Glasses: IL Futuro Della Tecnologia AR Per Occhiali Meta*. [Online]. Available: https://www.meta.com/it-it/emerging-tech/orion/2025

[3] *Meta AI Glasses*. Accessed: Apr. 9, 2025. [Online]. Available: https://www.ray-ban.com/usa/ray-ban-meta-ai-glasses

[4] (2024). *Smart Glasses Market By Type, Application, and Region-Global Forecast To 2028*. [Online]. Available: https://www.marketsandmarkets.com/Market-Reports/smart-glasses-market-148134046.html

[5] O. Amft, F. Wahl, S. Ishimaru, and K. Kunze, "Making regular eyeglasses smart," *IEEE Pervasive Comput.*, vol. 14, no. 3, pp. 32–43, Jul. 2015, doi: 10.1109/MPRV.2015.60.

[6] A. Ferlini, D. Ma, L. Qendro, and C. Mascolo, "Mobile health with head-Worn devices: Challenges and opportunities," *IEEE Pervasive Comput.*, vol. 21, no. 3, pp. 52–60, Jul. 2022, doi: 10.1109/MPRV.2022.3191711.

[7] J. Allen, "Photoplethysmography and its application in clinical physiological measurement," *Physiological Meas.*, vol. 28, no. 3, pp. R1–R39, Mar. 2007, doi: 10.1088/0967-3334/28/3/r01.

[8] P. H. Charlton et al., "Breathing rate estimation from the electrocardiogram and photoplethysmogram: A review," *IEEE Rev. Biomed. Eng.*, vol. 11, pp. 2–20, 2018, doi: 10.1109/RBME.2017.2763681.

[9] A. Scandelli, I. Crupi, P. Bartoli, A. Giudici, A. De Vecchi, and F. Villa, "Study of PPG sensor positioning on smart eyewear for biosensing," in *Proc. IEEE Sensors Appl. Symp. (SAS)*, Naples, Italy, Jul. 2024, pp. 1–6, doi: 10.1109/SAS60918.2024.10636483.

[10] Y. Zheng, B. Leung, S. Sy, Y. Zhang, and C. C. Y. Poon, "A clip-free eyeglasses-based wearable monitoring device for measuring photoplethysmograhic signals," in *Proc. Annu. Int. Conf. IEEE Eng. Med. Biol. Soc.*, San Diego, CA, USA, Aug. 2012, pp. 5022–5025, doi: 10.1109/EMBC.2012.6347121.

[11] N. Constant, O. Douglas-Prawl, S. Johnson, and K. Mankodiya, "Pulse-glasses: An unobtrusive, wearable HR monitor with Internet-of-Things functionality," in *Proc. IEEE 12th Int. Conf. Wearable Implant. Body Sensor Netw. (BSN)*, Cambridge, MA, USA, Jun. 2015, pp. 1–5, doi: 10.1109/BSN.2015.7299350.

[12] C. Holz and E. J. Wang, "Glabella: Continuously sensing blood pressure behavior using an unobtrusive wearable device," *Proc. ACM Interact., Mobile, Wearable Ubiquitous Technol.*, vol. 1, no. 3, pp. 1–23, Sep. 2017, doi: 10.1145/3132024.

[13] V. Toral-Lopez et al., "Wearable biosignal acquisition system for decision aid," *Proc. SPIE*, vol. 10662, pp. 69–77, May 2018, doi: 10.1117/12.2304988.

[14] N. Ahmed, R. Banerjee, A. Ghose, and A. Sinharay, "Feasibility analysis for estimation of blood pressure and heart rate using a smart eye wear," in *Proc. Workshop Wearable Syst. Appl.*, May 2015, pp. 9–14, doi: 10.1145/2753509.2753511.

[15] J. A. C. Patterson, D. C. McIlwraith, and G.-Z. Yang, "A flexible, low noise reflective PPG sensor platform for ear-Worn heart rate monitoring," in *Proc. 6th Int. Workshop Wearable Implant. Body Sensor Netw.*, Jun. 2009, pp. 286–291, doi: 10.1109/BSN.2009.16.

[16] N. Bui et al., "EBP: A wearable system for frequent and comfortable blood pressure monitoring from user's ear," in *Proc. 25th Annu. Int. Conf. Mobile Comput. Netw.*, Oct. 2019, pp. 1–17, doi: 10.1145/3300061.3345454.

[17] V. Chandel, A. Sinharay, N. Ahmed, and A. Ghose, "Exploiting IMU sensors for IoT enabled health monitoring," in *Proc. 1st Workshop IoT-enabled Healthcare Wellness Technol. Syst.*, Jun. 2016, pp. 21–22, doi: 10.1145/2933566.2933569.

[18] J. Windau and L. Itti, "Situation awareness via sensor-equipped eyeglasses," in *Proc. IEEE/RSJ Int. Conf. Intell. Robots Syst.*, Tokyo, Japan, Nov. 2013, pp. 5674–5679, doi: 10.1109/IROS.2013.6697178.

[19] A. Cristiano, A. Sanna, and D. Trojaniello, "Validity of a smart-glasses-based step-count measure during simulated free-living conditions," *Information*, vol. 11, no. 9, p. 404, Aug. 2020, doi: 10.3390/info11090404.

[20] A. De Vecchi, A. Scandelli, F. Bossi, B. C. Casadei, M. Boschi, and F. Villa, "On-the-edge gait analysis using a smart earable inertial measurement unit," in *Proc. IEEE Sensors Appl. Symp. (SAS)*, Naples, Italy, Jul. 2024, pp. 1–6, doi: 10.1109/SAS60918.2024.10636526.

[21] C. Floris et al., "Feasibility of heart rate and respiratory rate estimation by inertial sensors embedded in a virtual reality headset," *Sensors*, vol. 20, no. 24, p. 7168, Dec. 2020, doi: 10.3390/s20247168.

[22] T.-H. Hwang, J. Reh, A. O. Effenberg, and H. Blume, "Real-time gait analysis using a single head-Worn inertial measurement unit," *IEEE Trans. Consum. Electron.*, vol. 64, no. 2, pp. 240–248, May 2018, doi: 10.1109/TCE.2018.2843289.

[23] S. Ishimaru, K. Kunze, K. Tanaka, Y. Uema, K. Kise, and M. Inami, "Smart eyewear for interaction and activity recognition," in *Proc. 33rd Annu. ACM Conf. Extended Abstr. Human Factors Comput. Syst.*, Apr. 2015, pp. 307–310, doi: 10.1145/2702613.2725449.

[24] S. Solbiati et al., "Comparison of ECG-free algorithms for heart rate computation from head-BCG signals obtained with smart eyewear," in *Proc. IEEE Int. Conf. Metrology eXtended Reality, Artif. Intell. Neural Eng. (MetroXRAINE)*, Oct. 2024, pp. 213–218, doi: 10.1109/METROXRAINE62247.2024.10795866.

[25] M. Dhuliawala et al., "Smooth eye movement interaction using EOG glasses," in *Proc. 18th ACM Int. Conf. Multimodal Interact.*, Oct. 2016, pp. 307–311, doi: 10.1145/2993148.2993181.

[26] N. Kosmyna, C. Morris, U. Sarawgi, T. Nguyen, and P. Maes, "AttentivU: A wearable pair of EEG and EOG glasses for real-time physiological processing," in *Proc. IEEE 16th Int. Conf. Wearable Implant. Body Sensor Netw. (BSN)*, Chicago, IL, USA, May 2019, pp. 1–4, doi: 10.1109/BSN.2019.8771080.

[27] R. Zhang and O. Amft, "Monitoring chewing and eating in free-living using smart eyeglasses," *IEEE J. Biomed. Health Informat.*, vol. 22, no. 1, pp. 23–32, Jan. 2018, doi: 10.1109/JBHI.2017.2698523.

[28] C. C. Kim, J. Han, D. Zheng, G. Chernyshov, and K. Kunze, "Using smart eyewear to sense electrodermal activity while reading," in *Proc. ACM Int. Joint Conf. Pervasive Ubiquitous Comput. Proc. ACM Int. Symp. Wearable Comput.*, Sep. 2021, pp. 472–475, doi: 10.1145/3460418.3479356.

[29] M. N. Saadatzi, F. Tafazzoli, K. C. Welch, and J. H. Graham, "EmotiGO: Bluetooth-enabled eyewear for unobtrusive physiology-based emotion recognition," in *Proc. IEEE Int. Conf. Autom. Sci. Eng. (CASE)*, Fort Worth, TX, USA, Aug. 2016, pp. 903–909, doi: 10.1109/COASE.2016.7743498.

[30] Siddharth, A. N. Patel, T.-P. Jung, and T. J. Sejnowski, "A wearable multi-modal bio-sensing system towards real-world applications," *IEEE Trans. Biomed. Eng.*, vol. 66, no. 4, pp. 1137–1147, Apr. 2019, doi: 10.1109/TBME.2018.2868759.

[31] J. Nie et al., "SPIDERS+: A light-weight, wireless, and low-cost glasses-based wearable platform for emotion sensing and bio-signal acquisition," *Pervas. Mobile Comput.*, vol. 75, Aug. 2021, Art. no. 101424, doi: 10.1016/j.pmcj.2021.101424.

[32] M. S. Islam, T. Hossain, M. A. R. Ahad, and S. Inoue, "Exploring human activities using eSense earable device," in *Activity and Behavior Computing* (Smart Innovation, Systems and Technologies), vol. 204, M. A. R. Ahad, S. Inoue, D. Roggen, and K. Fujinami, Eds., Singapore: Springer, 2021, doi: 10.1007/978-981-15-8944-7_11.

[33] G. Ouyang and K. Abed-Meraim, "Analysis of magnetic field measurements for indoor positioning," *Sensors*, vol. 22, no. 11, p. 4014, May 2022, doi: 10.3390/s22114014.

[34] A. Manivannan, W. C. B. Chin, A. Barrat, and R. Bouffanais, "On the challenges and potential of using barometric sensors to track human activity," *Sensors*, vol. 20, no. 23, p. 6786, Nov. 2020, doi: 10.3390/s20236786.

[35] L. Neri et al., "Electrocardiogram monitoring wearable devices and artificial-intelligence-enabled diagnostic capabilities: A review," *Sensors*, vol. 23, no. 10, p. 4805, May 2023, doi: 10.3390/s23104805.

[36] D. J. C. Matthies, A. Woodall, and B. Urban, "Prototyping smart eyewear with capacitive sensing for facial and head gesture detection," in *Proc. ACM Int. Joint Conf. Pervasive Ubiquitous Comput. Proc. ACM Int. Symp. Wearable Comput.*, Sep. 2021, pp. 476–480, doi: 10.1145/3460418.3479361.

[37] V. Sakthivelpathi et al., "Capacitive eye tracker made of fractured carbon nanotube-paper composites for wearable applications," *Sens. Actuators A, Phys.*, vol. 344, Sep. 2022, Art. no. 113739, doi: 10.1016/j.sna.2022.113739.

[38] G. Ma, W. Zhu, J. Zhong, T. Tong, J. Zhang, and L. Wang, "Wearable ear blood oxygen saturation and pulse measurement system based on PPG," in *Proc. IEEE SmartWorld, Ubiquitous Intell. Comput., Adv. Trusted Comput., Scalable Comput. Commun., Cloud Big Data Comput., Internet People Smart City Innov. (SmartWorld/SCALCOM/UIC/ATC/CBDCom/IOP/SCI)*, Guangzhou, China, Oct. 2018, pp. 111–116, doi: 10.1109/SMARTWORLD.2018.00054.

[39] I. Crupi, A. Scandelli, A. Giudici, and F. Villa, "Development of a miniaturized, low-power, head-mounted PCB for continuous PPG monitoring and real- time HR estimation," in *Proc. IEEE Sensors Appl. Symp. (SAS)*, Naples, Italy, Jul. 2024, pp. 1–5, doi: 10.1109/SAS60918.2024.10636362.

[40] A. C. Palmisciano et al., "Eyewear-based ECG recording: A novel head-electrode approach for reliable cardiac signal acquisition," *IEEE Access*, vol. 13, pp. 45488–45499, 2025, doi: 10.1109/ACCESS.2025.3547230.

Ilaria Crupi (Graduate Student Member, IEEE) received the M.Sc. degree in biomedical engineering from the Politecnico di Milano, Milan, Italy, in 2023. She is currently pursuing the Ph.D. degree in information technology (electronics) with the Smart Eyewear Laboratory, a Joint Research Center between Politecnico di Milano and EssilorLuxottica, Milan.

Her research focuses on the development of integrated hardware and firmware solutions for extracting cardiovascular parameters from the head. In particular, she works on low-power electronic systems design, embedded firmware development, and signal processing techniques for photoplethysmography-based monitoring.

Alice Scandelli (Graduate Student Member, IEEE) received the bachelor's and master's degrees in biomedical engineering from the Politecnico di Milano, Milan, Italy, in 2020 and 2022, respectively. She is currently pursuing the Ph.D. degree in information technology with the Smart Eyewear Laboratory, a Joint Research Center between Politecnico di Milano and EssilorLuxottica, Milan.

Her research focuses on the design of low-power, multisensor wearable systems for real-time cardiorespiratory monitoring, aiming to advance wearable technologies through innovative design and embedded data processing.

Andrea Giudici (Member, IEEE) received the master's degree in electronics engineering and the Ph.D. degree in information and communication technology from the Politecnico di Milano, Milan, Italy, in 2019 and 2022, respectively, with a focus on the design of readout integrated electronics for single-photon avalanche diodes (SPADs) targeting LiDAR and time-correlated single-photon counting (TCSPC) applications.

His current research interests include the design and development of electronic systems for health monitoring and computer vision applications.

Giacomo Gervasoni received the B.Sc. degree in biomedical engineering and the M.Sc. and Ph.D. degrees in electronics engineering from the Politecnico di Milano, Milan, Italy, in 2011, 2013, and 2016, respectively.

During his Ph.D., he worked on the design and development of a high-resolution lock-in amplifier. He has industry experience in biomedical devices and scientific X-ray fluorescence (XRF) instrumentation. He is currently a Principal Researcher with EssilorLuxottica, Milan, and conducts research within the Smart Eyewear Laboratory, a Joint Research Center between EssilorLuxottica and Politecnico di Milan, focusing on efficient sensing and processing electronics for smart eyewear.

Diana Trojaniello received the Ph.D. degree in bioengineering from the Alma Mater Studiorum University of Bologna, Bologna, Italy, in 2015.

She worked as the Head of Bioengineering Research Program. Since 2021, she has been the Deputy Director with the Center for Advanced Technology in Health and Wellbeing with San Raffaele Hospital, Milan, Italy. She is currently the Camera and Sensor Stream Research Manager with the EssilorLuxottica Smart Eyewear Laboratory, Milan, and an Adjunct Professor with the University Vita-Salute San Raffaele, Milan. Passionate about innovative tech-enabled solutions for the healthcare and wellbeing sector, with more than ten years of experience in international research and development projects management in the area of wearable devices and digital health.

Federica Villa (Member, IEEE) was born in Milan, Italy, in 1986. She received the master's (summa cum laude) degree in electronics engineering and the Ph.D. degree in information and communication technology from the Politecnico di Milano, Milan, in 2010 and 2014, respectively.

Since 2021, she has been an Associate Professor with the Politecnico di Milano. She has co-authored 184 articles, and her H-index is 32. Her present research activities include the design and development of sensor systems for health monitoring and for bioimaging with super-resolution and quantum techniques.